Application of Local Splines for Solving Integral Equations of Several Variables

I. G. BUROVA, G. O. ALCYBEEV, S. A. SHIPCOVA
Computational Mathematics Department
St.Petersburg State University
7/9 Universitetskaya nab. St. Petersburg, 199034
RUSSIA

Abstract: - The proposed approximation of a function of several variables is based on the direct product of local splines of one variable. The approximation is built on each elementary parallelepiped separately and is reduced to calculating the sum of the products of the function values and the basis splines. The use of non-polynomial basis splines with different properties in different directions allows us to obtain a qualitatively better approximation. Solving the Fredholm integral equation of the second kind of several variables is reduced to calculating the integrals of the product of the kernel and the basis splines and solving a system of linear algebraic equations. A comparison of the results of the numerical solution of integral equations by the proposed method and the results of applying other methods is given.

Key-Words: Fredholm Integral equations of the second kind, Local splines, Nonpolynomial splines, Approximation, Interpolation, Several Variables

Received: April 19, 2025. Revised: August 16, 2025. Accepted: September 19, 2025. Published: June 1, 2026.

1 Introduction

When studying various physical processes, mathematical linear or nonlinear models are constructed, based on linear or nonlinear differential equations, including partial differential equations. There is a need to develop new numerical methods for solving boundary value problems, the Cauchy problem (see, [1], [2], [3]). Particularly relevant in the development of numerical methods is the use of finite elements, [4], various types of wavelets, [5], [6], splines [6], [7], [8]. In many cases, solving boundary value problems and the Cauchy problem is reduced to solving an integral equation. Fredholm integral equations have applications in plasma physics, electrical engineering, [9], telegraph equations, [10], and in many other directions of applied physics and mathematics. Integral equations can be solved using numerical quadrature and cubature formulas. The numerical quadrature and cubature formulas are given, for example, in [11].

Integral equations are a useful tool for a large number of modeling problems that arise in computer graphics, manipulations, aerodynamics, fracture mechanics, and electromagnetic scattering, [12], [13]. The historical development of integral equations is closely related to the solutions of boundary value problems. Generally, the boundary value problems of the differential equations are converted to integral equations, [14], [15]. For example, the Laplace equation of boundary conditions is reduced to a Fredholm integral equation of the second kind by the direct boundary element method, [15]. Nowadays, when solving linear Fredholm equations, calculation schemes are constructed in different ways, for example, by combining the meshless barycentric Lagrange interpolation functions and the Gauss-Legendre quadrature formula, [16]. In paper, [17], an algorithm is developed for solving two-dimensional linear Fredholm integral equations of the second kind by the integral mean value theorem. In the proposed numerical method, each element of the generated discrete matrix does not required to calculate integrals, and the approximate integral operator is convergent according to the collectively compact theory. In paper, [18], numerical solution methods for two-dimensional Fredholm integral equations of the second kind are considered.

Suppose $f(x,y)$ and $K(x,y,s,t)$ are given continuous functions defined on $D=[a,b]\times[a,b]$. In this paper, we consider the following linear integral equation.

$$u(x,y)-\int_a^b\int_a^b K(x,y,s,t)u(s,t)dsdt=f(x,y),$$

where $u(x,y)$ is an unknown function in D.

2 Spline interpolation method

2.1 Second-order splines of approximation with one variable

The construction of local spline approximations of one variable has been studied in [19]. The estimations of the errors of approximating by non-polynomial splines can be obtained following the method described in paper, [19]. A grid of ordered nodes $\{x_j\}$ is given with a step $h_j=x_{j+1}-x_j$ on $[a,b]$: $a=x_0<\ldots<x_n=b, n\geq 1$.

Approximation $U(s)$ using second-order approximation basis splines of one variable on one grid interval $[x_k,x_{k+1}]$ is constructed in the following form:

$$U(s)=u(x_k)\omega_k(s)+u(x_{k+1})\omega_{k+1}(s),\quad s\in[x_k,x_{k+1}].$$

We assume that the support of the basis spline $\omega_k(s)$ occupies two grid intervals:

$$supp\ \omega_k=[x_{k-1},x_{k+1}].$$

Suppose the functions $\varphi_0(s),\varphi_1(s)$ form a Chebyshev system on the interval $[x_k,x_{k+1}]$. Basis splines on the interval $[x_k,x_{k+1}]$ are found from the condition:

$$U(s)=u(s), u\ (s)=\varphi_0(s),\varphi_1(s).$$

Thus, we arrive at a system of approximation identities.

$$\varphi_0(x_k)\omega_k(s)+\varphi_0(x_{k+1})\omega_{k+1}(s)=\varphi_0(s),$$
$$\varphi_1(x_k)\omega_k(s)+\varphi_1(x_{k+1})\omega_{k+1}(s)=\varphi_1(s),$$
$$s\in[x_k,x_{k+1}].$$

From here, we obtain the formulas for basis splines

$$\omega_k(s)=\frac{\varphi_0(s)\varphi_1(x_{k+1})-\varphi_1(s)\varphi_0(x_{k+1})}{\varphi_1(x_{k+1})\varphi_0(x_k)-\varphi_1(x_k)\varphi_0(x_{k+1})},\quad s\in[x_k,x_{k+1}],$$
$$\omega_{k+1}(s)=\frac{\varphi_0(s)\varphi_1(x_k)-\varphi_1(s)\varphi_0(x_k)}{\varphi_1(x_k)\varphi_0(x_{k+1})-\varphi_1(x_{k+1})\varphi_0(x_k)},\quad s\in[x_k,x_{k+1}].$$

Next, we can obtain special cases of basis splines. If $\varphi_0(s)=1,\varphi_1(s)=s$, then we obtain formulas for polynomial basis splines

$$\omega_k^p(s)=\begin{cases}\dfrac{s-x_{k+1}}{x_k-x_{k+1}}, & s\in[x_k,x_{k+1}],\\ \dfrac{s-x_{k-1}}{x_k-x_{k-1}}, & s\in[x_{k-1},x_k],\end{cases}$$
$$\omega_k^p(s)=0 \text{ when } s\notin[x_{k-1},x_{k+1}].$$

In addition, we give the formula of $\omega_{k+1}(s)$:

$$\omega_{k+1}^p(s)=\frac{s-x_k}{x_{k+1}-x_k},\quad s\in[x_k,x_{k+1}].$$

The plot of the polynomial basis splines has a support consisting of two grid intervals and is shown in Figure 1a. The error of the approximation can be given by the relation, [19]:

$$|u(s)-U(s)|\leq\frac{1}{8}h^2\parallel u''\parallel_{C[x_k,x_{k+1}]}.$$

If $\varphi_0=\sin(s),\varphi_1=\cos(s)$, then we obtain formulas for the trigonometric basis spline:

$$\omega_k^T(s)=\frac{\sin(s-x_{k+1})}{\sin(x_k-x_{k+1})},\quad s\in[x_k,x_{k+1}],$$
$$\omega_{k+1}^T(s)=\frac{\sin(s-x_k)}{\sin(x_{k+1}-x_k)},\quad s\in[x_k,x_{k+1}].$$
$$\omega_k^T(s)=0 \text{ when } s\notin[x_{k-1},x_{k+1}].$$

The support of the trigonometric basis spline consists of two grid intervals. The plot of the trigonometric basis spline is shown in Figure 1b.
The error of the approximation can be given by the relation:

$$|u(s)-U(s)|\leq Kh^2\parallel u+u''\parallel_{C[x_k,x_{k+1}]},\quad K=\text{const}.$$

If $\varphi_0=1,\varphi_1(s)=e^s$, then we obtain formulas for the exponential basis splines ω_k^{ep}, $\omega_{k+1}^{ep}(s)$ in the following form:

$$\omega_k^{ep}(s)=\frac{e^s-e^{x_{k+1}}}{e^{x_k}-e^{x_{k+1}}},\quad s\in[x_k,x_{k+1}],$$
$$\omega_{k+1}^{ep}(s)=\frac{e^s-e^{x_k}}{e^{x_{k+1}}-e^{x_k}},\quad s\in[x_k,x_{k+1}].$$
$$\omega_k^{ep}(s)=0 \text{ when } s\notin[x_{k-1},x_{k+1}].$$

The error of the approximation with the exponential basis splines can be given by the relation, [19]:

$$|u(s)-U(s)|\leq Kh^2\parallel u+u''\parallel_{C[x_k,x_{k+1}]},$$
$K=$ const.
The plot of the exponential basis spline is shown in Figure 1c.

The error of the approximation can be given by the relation:
$|u(s) - U(s)| \leq Kh^2 e^{x_{k+1}} \parallel u'' - u \parallel_{C[x_k, x_{k+1}]}$,
$K = \text{const}$.

If $\varphi_0 = 1, \varphi_1(s) = e^{-s}$, then we obtain formulas for the exponential basis splines in the form:

$$\omega_k^{eo}(s) = \frac{e^{-s} - e^{-x_{k+1}}}{e^{-x_k} - e^{x_{k+1}}}, \quad s \in [x_k, x_{k+1}],$$

$$\omega_{k+1}^{eo}(s) = \frac{e^{-s} - e^{-x_k}}{e^{-x_{k+1}} - e^{-x_k}}, \quad s \in [x_k, x_{k+1}].$$

$$\omega_k^{eo}(s) = 0 \text{ when } s \notin [x_{k-1}, x_{k+1}].$$

The error of the approximation can be given by the relation:
$|u(s) - U(s)| \leq Kh^2 \exp(x_k) \parallel u'' - u \parallel_{C[x_k, x_{k+1}]}$,
$K = \text{const}$.

The plot of the exponential basis splines is shown in Figure 1d.

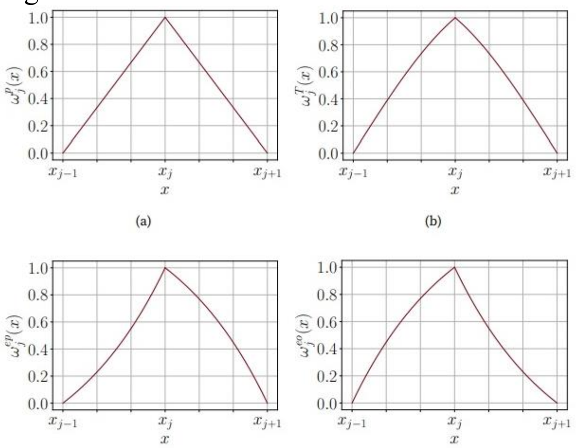

Fig. 1. The plots of different types of basis splines: a) polynomial; b) trigonometric; c) exponential; d) exponential.
Source: created by the authors

Let us present the results of the approximation of some functions $u(x)$ using polynomial and nonpolynomial splines on $[a, b] = [-1, 1]$. The approximations were constructed on a uniform grid of nodes with $h = (b - a)/n$.
In Table 1 and Table 2, the actual values of approximation errors are given. The maximum absolute values of the actual errors in the approximation of the functions:

$$\tilde{R} = \max_{k=0,\ldots,n-1} \max_{x \in [x_k, x_{k+1}]} |u(x) - U(x)|$$

Table 1 shows the values of the actual errors $\tilde{R}$ when $n = 20$. Table 2 shows the values of the actual errors $\tilde{R}$, $n = 200$. The calculations were performed in the Maple system with $Digits = 10$.

Table 1. Actual values of approximation errors of some functions $\tilde{R}$ obtained using polynomial and non-polynomial splines when $a = -1, b = 1, n = 20$

$u(x)$	$\varphi_0 = 1$, $\varphi_1 = x$	$\varphi_0 = 1$, $\varphi_1 = e^x$	$\varphi_0 = 1$, $\varphi_1 = e^{-x}$	$\varphi_0 = \sin(x)$, $\varphi_1 = \cos(x)$
1	0	0	0	$0.13 \cdot 10^{-2}$
e^x	$0.32 \cdot 10^{-2}$	0	$0.65 \cdot 10^{-2}$	$0.65 \cdot 10^{-2}$
e^{-x}	$0.32 \cdot 10^{-2}$	$0.65 \cdot 10^{-2}$	0	$0.65 \cdot 10^{-2}$
x	0	$0.13 \cdot 10^{-2}$	$0.13 \cdot 10^{-2}$	$0.12 \cdot 10^{-2}$
$\sin(x)$	$0.10 \cdot 10^{-2}$	$0.18 \cdot 10^{-2}$	$0.18 \cdot 10^{-2}$	$0.17 \cdot 10^{-10}$
$\cos(x)$	$0.10 \cdot 10^{-2}$	$0.18 \cdot 10^{-2}$	$0.18 \cdot 10^{-2}$	$0.18 \cdot 10^{-10}$
$(1 + 25x^2)^{-1}$	$0.41 \cdot 10^{-2}$	$0.44 \cdot 10^{-2}$	$0.44 \cdot 10^{-2}$	$0.41 \cdot 10^{-2}$

Source: created by the authors

Table 2 Actual errors $\tilde{R}$ obtained using polynomial and non-polynomial splines when $a = -1, b = 1, n = 200$, Digits=10

$u(x)$	$\varphi_0 = 1$, $\varphi_1 = x$	$\varphi_0 = 1$, $\varphi_1 = e^x$	$\varphi_0 = 1$, $\varphi_1 = e^{-x}$	$\varphi_0 = \sin(x)$, $\varphi_1 = \cos(x)$
1	0	0	0	$0.13 \cdot 10^{-4}$
e^x	$0.33 \cdot 10^{-4}$	0	$0.68 \cdot 10^{-4}$	$0.68 \cdot 10^{-4}$
e^{-x}	$0.33 \cdot 10^{-4}$	$0.68 \cdot 10^{-4}$	0	$0.68 \cdot 10^{-4}$
x	0	$0.13 \cdot 10^{-4}$	$0.13 \cdot 10^{-4}$	$0.12 \cdot 10^{-4}$
$\sin(x)$	$0.10 \cdot 10^{-4}$	$0.18 \cdot 10^{-4}$	$0.18 \cdot 10^{-4}$	$0.16 \cdot 10^{-10}$
$\cos(x)$	$0.10 \cdot 10^{-4}$	$0.18 \cdot 10^{-4}$	$0.18 \cdot 10^{-4}$	$0.18 \cdot 10^{-10}$
$(1 + 25x^2)^{-1}$	$0.62 \cdot 10^{-3}$	$0.63 \cdot 10^{-3}$	$0.63 \cdot 10^{-3}$	$0.61 \cdot 10^{-3}$

Source: created by the authors

The results presented in Table 1 and Table 2 are consistent with theoretical estimates of errors.

2.1 Method for approximation functions of two variables

Now, we discuss the spline interpolation method for approximation functions of two variables. Suppose a continuous function of two variables is defined in a rectangular region G, and the second derivative of the function for each of these variables is bounded. We begin by constructing a rectangular grid of nodes in this region G.
A rectangular grid of ordered equidistant nodes $\{x_i\}$ and $\{y_j\}$ is given with steps

$$h_x = x_{i+1} - x_i, \;\; i = 0, \ldots, n-1,$$
$$h_y = y_{j+1} - y_j, \;\; j = 0, \ldots, m-1,$$

on a rectangular region $G = [a, b] \times [c, d]$:

$$a = x_0 < x_1 < \cdots < x_n = b, \;\; c = y_0 < y_1 < \cdots < y_m = d, \;\; n, m \geq 1.$$

Suppose the values of the function $u(x_i, y_j)$ are given at the grid nodes. Suppose Π_{ij} denotes the elementary parallelepiped (Figure 2):

$$\Pi_{ij} = [x_i, x_{i+1}] \times [y_j, y_{j+1}].$$

In each elementary parallelepiped Π_{ij} with vertices at the points
$(x_i, y_j), (x_{i+1}, y_j), (x_i, y_{j+1}), (x_{i+1}, y_{j+1})$
we construct the approximation $U_{ij}(x,y)$ with the basis splines, using direct production of one-dimensional basis functions $\omega_i(x)$ and $\omega_j(y)$ according to the next rule:

$$U_{ij}(x,y) = u_{ij}\Omega_{ij}(x,y) + u_{i+1,j}\Omega_{i+1,j}(x,y) + u_{i,j+1}\Omega_{i,j+1}(x,y) + u_{i+1,j+1}\Omega_{i+1,j+1}(x,y),$$
$$x \in [x_i, x_{i+1}],\ \ y \in [y_j, y_{j+1}],$$
$$i = 0,1,\dots,n-1, \qquad j = 0,1,\dots,m-1,$$

where
$$\Omega_{ij}(x,y) = \omega_i(x)\omega_j(y),\ \ i = 0,1,\dots,n-1,\ \ j = 0,1,\dots,m-1.$$

The plot of the polynomial basis splines of two variables (a polynomial spline in the direction of the axis X and a polynomial spline in the direction of the axis Y) is given in Figure 3a. The plot of the trigonometric basis splines of two variables (a trigonometric spline in the direction of the axis X and a trigonometric spline in the direction of the axis Y) is given in Figure 3b.

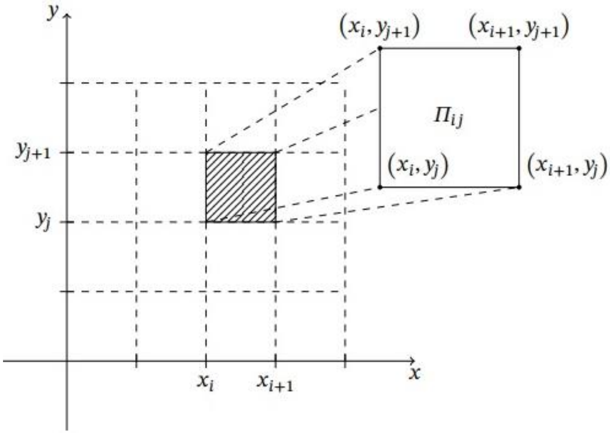

Fig. 2. The mesh and the elementary parallelepiped Π_{ij}.
Source: created by the authors

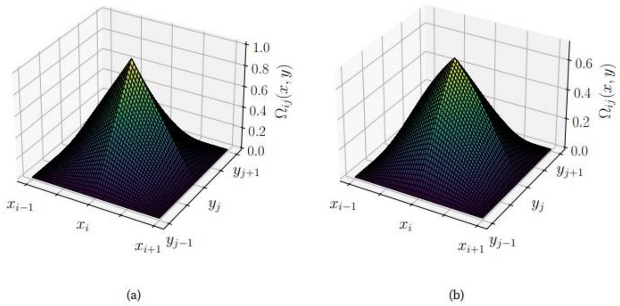

Fig. 3. The plots of the basis splines of two variables: a) polynomial; b) trigonometric.
Source: created by the authors

We denote the derivatives of a function of two variables as follows:
$$D^{r,s}f(x,y) = \frac{\partial^{r+s}f(x,y)}{\partial x^r \partial y^s}.$$

Theorem. Suppose $u \in C^2[\Pi_{ij}]$. For $(x,y) \in \Pi_{ij}$ in the case of local polynomial approximations of the first degree, we have the estimate:

$$|u(x,y) - U_{ij}(x,y)| \le \frac{1}{8}h_x^2 \parallel D^{2,0}u \parallel_{C[\Pi_{ij}]} + \frac{1}{8}h_y^2 \parallel D^{0,2}u \parallel_{C[\Pi_{ij}]}$$

Proof.
First, note that $U_{ij}(x,y) = u(x,y)$, if $u = 1, x, y$, and $(x,y) \in \Pi_{ij}$. Expanding the functions $u(x,y), U_{ij}(x,y)$ using the Taylor formula in the neighborhood of the point (x_i, y_j), taking into account the approximation identities for the case of one variable, we obtain the error estimate specified in the formulation of the theorem.

Note. Using a similar method for other variants of approximations with the polynomial and non-polynomial splines, we obtain the error estimate $O(h_x^2 + h_y^2)$ for $(x,y) \in \Pi_{ij}$.

3 Application of splines to the solution of the Fredholm integral equation of the second kind

Next, for convenience, we consider a square region G and the same number of nodes $(n = m)$ in this region, both along the X-axis and along the Y-axis.
Consider the Fredholm integral equation of the second kind
$$u(x,y) - \int_a^b \int_a^b K(x,y,s,t)u(s,t)dsdt = f(x,y),$$
$$(x,y) \in ([a,b] \times [a,b])$$
We suppose that the kernel $K(x,y,s,t)$ and function $f(x,y)$ are the continuous functions.
Now we can represent the integral
$$\int_a^b \int_a^b K(x,y,s,t)u(s,t)dsdt$$
as a sum of the following form:
$$\sum_{i=0}^{n-1}\sum_{j=0}^{n-1}\int_{x_i}^{x_{i+1}}\int_{y_j}^{y_{j+1}} K(x_l,y,s,t)u(s,t)dsdt\,.$$
Next, we replace the function $u(s,t)$ with $U(s,t)$. Thus, we receive the following integral equation:
$$u(x_l, y_k) +$$

$$\sum_{i=0}^{n-1}\sum_{j=0}^{n-1}\int_{x_i}^{x_{i+1}}\int_{y_j}^{y_{j+1}}K(x_l,y_k,s,t)U(s,t)dsdt = f(x_l,y_k)+R,$$

where R is a remainder term.

Finally, we have to solve the system of equations

$$u(x_l,y_k)+\sum_{i=0}^{n-1}\sum_{j=0}^{n-1}\int_{x_i}^{x_{i+1}}\int_{y_j}^{y_{j+1}}K\big(x_l,y_k,s,t\big)U(s,t)dsdt = f(x_l,y_k),$$

$l,k,i,j=0,\dots,n-1$.

During the solution, we have to calculate the integrals

$$V_{ij\alpha\beta}=\int_{x_i}^{x_{i+1}}\int_{y_j}^{y_{j+1}}K\big(x_l,y_k,s,t\big)\Omega_{i+\alpha\, j+\beta}(s,t)dsdt,$$

$\alpha,\beta=0,1$.

The advantages of this method include the ease of use of an adaptive non-uniform grid, and the ability to apply different types of spline approximations (exponential or trigonometric) along axis X or axis Y.

3.1. The cubature method for solving integral equations

The cubature method for solving integral equations of two variables is well known. We assume that the kernel and right-hand side are continuous functions.

We consider a multiple integral over a rectangular region

$$\iint_G g(x,y)dxdy=\int_a^b dx\int_a^b g(x,y\,)dy.$$

We can successively apply, for example, the trapezoidal rule to the iterated integral. Applying the quadrature rule to the inner integral, we obtain

$$\int_a^b\int_a^b g(x,y\,)dxdy=\sum_{i=0}^{n-1}a_i\int_a^b g(x_i,y)dy+R_n,$$

where R_n is the remainder term, a_i is the quadrature coefficient, x_i are the nodes of the quadrature rule.

Next we get

$$\int_a^b g(x_i,y)dy=\sum_{j=0}^{n-1}b_j g\big(x_i,y_j\big)+r_n,$$

where r_n is the remainder term, b_j is the quadrature coefficient, y_j are the nodes of the quadrature rule.

Then the integral

$$\int_a^b\int_a^b g(x,y\,)dxdy=\sum_{i=0}^{n-1}\sum_{j=0}^{n-1}C_{ij}\ g\big(x_i,y_j\big)+R,$$

where $C_{ij}=a_i b_j$,

$$R=R_n+\sum_{i=0}^{n-1}a_i r_n\,.$$

We apply the above relations to the calculation of integral equations of the second kind:

$$z(x,y)-\int_a^b\int_a^b K(x,y,s,t)z(s,t\,)dxdy=f(x,y).$$

Here, we assume the continuity of the kernel and the right-hand side. We take a grid of nodes (s_i,t_j) where $i,j=0,1,\dots,n-1$. The integral is replaced by cubature formulas for fixed x,y .

$$z(x,y)-\sum_{j=0}^{n-1}\sum_{i=0}^{n-1}C_{ij}\,K\big(x,y,s_i,t_j\big)z(x,y)+R = f(x,y).$$

Next, we take a grid of nodes (x_p,y_k) in the region G, where $p,k=0,\ 1,\dots,\ n-1$.

Here, we assume the continuity of the kernel and the right-hand side. The integral is replaced by cubature formulas for fixed x,y .

We obtain:

$$z(x_p,y_k)-\sum_{j=0}^{n-1}\sum_{i=0}^{n-1}C_{ij}\,K\big(x_p,y_k,s_i,t_j\big)z(x,y)+R = f(x_p,y_k).$$

Discarding the error, we obtain the equations for approximately finding the solution to the integral equation:

$$z_{pk}-\sum_{j=0}^{n-1}\sum_{i=0}^{n-1}C_{ij}\,K\big(x_p,y_k,s_i,t_j\big)z_{ij}=f_{pk},$$

where

$$z_{pk}\ \approx z(x_p,y_k).$$

Here we have a 4-index matrix, which we expand into a 2-index matrix and a vector (for the right-hand side). We expand the matrix (z_{pk}) into a column vector by assigning the second column to the first, the third to the second, and so on for $p,k=0,1,..,n-1$. The indices (p,k) are transformed into indices $q=p\,n+k$, respectively. Then $q=0,1,..n^2-1$, and the matrix (z_{pk}) is transformed into a vector $Z=(z_q)$, where $z_q=z(x_p,y_k)$.

Thus, we write the double sum as the product of a matrix row and a vector Z of unknowns z_q, which we represent as the vector of matrix unfolding (z_{pk}) into a vector.

Next, we unfold the 4-index matrix $K(x_p,y_k,s_i,t_j)$ into a regular matrix so that the indices (i,j) correspond to the indices q of the vector $z=(z_q)$.

From here, we obtain the matrix $M = (M_{qn})$:

$$M_{qn} = K(x_p, y_k, s_i, t_j) A_i B_j$$

Then we have a system of linear algebraic equations of the form:

$$z - Mz = F,$$

where vectors $z = (z_q)$ and $F = (F_q)$.

3.2. Spline method application

When using the spline method, we get the system of equations

$$u_{pk} - \sum_{i=0}^{n-1} \sum_{j=0}^{n-1} C_{ij} u_{ij} = f_{pk}$$

where $u_{ij} \approx u(s_i, t_j)$ at nodes.

The coefficients of the matrix C_{ij} are as follows. For all interior points of the region G, we have the coefficients for $u_{i+1\,j+1}$:

$$\int_{s_i}^{s_{i+1}} \int_{t_j}^{t_{j+1}} K(x_p, y_k, s, t) \Omega_{i+1\,j+1}(s,t) ds dt +$$

$$\int_{s_{i+1}}^{s_{i+2}} \int_{t_j}^{t_{j+1}} K(x_p, y_k, s, t) \Omega_{i+1\,j+1}(s,t) ds dt +$$

$$\int_{s_i}^{s_i} \int_{t_{j+1}}^{t_{j+2}} K(x_p, y_k, s, t) \Omega_{i+1\,j+1}(s,t) ds dt +$$

$$\int_{s_{i+1}}^{s_{i+2}} \int_{t_{j+1}}^{t_{j+2}} K(x_p, y_k, s, t) \Omega_{i+1\,j+1}(s,t) ds dt.$$

For boundary points (but not corner points of the region) G, we have relations of the form: For example, the coefficient for $u_{i\,j+1}$ is as follows:

$$\int_{s_i}^{s_{i+1}} \int_{t_j}^{t_{j+1}} K(x, y, s, t) \Omega_{i\,j+1}(s,t) ds dt +$$

$$\int_{s_i}^{s_{i+1}} \int_{t_{j+1}}^{t_{j+2}} K(x, y, s, t) \Omega_{i\,j+1}(s,t) ds dt.$$

The coefficient for $u_{i+1\,j}$ is as follows:

$$\int_{s_i}^{s_{i+1}} \int_{t_j}^{t_{j+1}} K(x, y, s, t) \Omega_{i+1\,j}(s,t) ds dt +$$

$$\int_{s_{i+1}}^{s_{i+2}} \int_{t_{j+1}}^{t_{j+2}} K(x, y, s, t) \Omega_{i+1\,j}(s,t) ds dt.$$

The coefficients of the unknowns for the corner nodes contain one integral term, for example, the coefficient of u_{00} is the following:

$$\int_{s_0}^{s_0} \int_{t_0}^{t_0} K(x, y, s, t) \Omega_{0\,0}(s,t) ds dt.$$

Next, using the method described above, we obtain a system of linear algebraic equations.

Thus, we have the vector $u = (u_q)$, where u_q is its component and the index $q = pn + k$. Here, the change in index is as follows: $q = 0, 1, \ldots, n^2 - 1$.
Denote A the matrix of the system of equations.
We obtain a system of equations of the form

$$Au = F.$$

The matrix A of the system of equations is filled. Using the theorem on approximation error, we obtain an estimate of the error in solving the integral equation on an equidistant grid of nodes is as follows $O(h_x^2 + h_y^2)$.
It is useful to find the condition number of matrix A for various variants of the basis splines. As is well known, the condition number is calculated as follows

$$cond\,(A) = \parallel A \parallel \parallel A^{-1} \parallel.$$

The condition numbers of the matrix are presented in the numerical examples below.

4 Numerical experiments

In this section, we consider the results of applying the spline method to solving integral equations from some recently published papers.

Example 1. Consider the integral equation from paper, [20]

$$2u(x,y) + \int_0^{1.1} \int_0^{1.1} e^{x+y-s-t} u(s,t) ds dt = 3.21 e^{x+y},$$

where $u(x, y) = \exp(x + y)$ is the exact solution.
We take $n = 4$ and construct a set of nodes along the X and Y axes, a total of 25 nodes.
We denote $R_{ij} = u(x_i, y_j) - U(x_i, y_j)$.
The following figures show the errors in the solutions of the integral equation obtained in the Maple program for different parameter Digits values.
Figure 4, Figure 5, and Figure 6 show the errors of the solution at points (x_i, R_{ij}), when $i, j = 0, 1, 2, 3, 4$. Along axes Y, the errors of the solution are given at point (x_i, y_j), along axes X the points x_i are given.
Figure 4 shows the errors when $j = 1$ (red), $j = 2$ (blue), and $j = 3$ (gold) points when using basis polynomial splines, n =4, Digits=15.
Figure 5 shows the errors when n =4, Digits=15.

Figure 6 shows the errors when n =8, Digits=20.

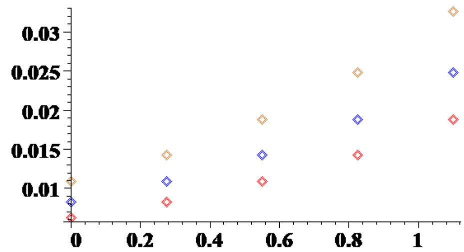

Fig. 4. The errors of the approximate solution at the nodes when we use polynomial splines, n =4, Digits=15.
Source: created by the authors

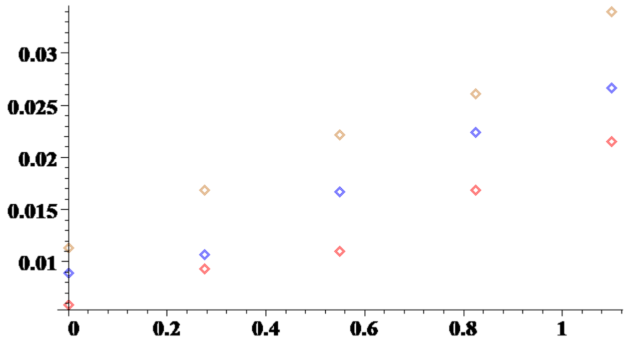

Fig. 5. The errors of the approximate solution at the nodes when we use polynomial splines, n = 4, Digits=5.
Source: created by the authors

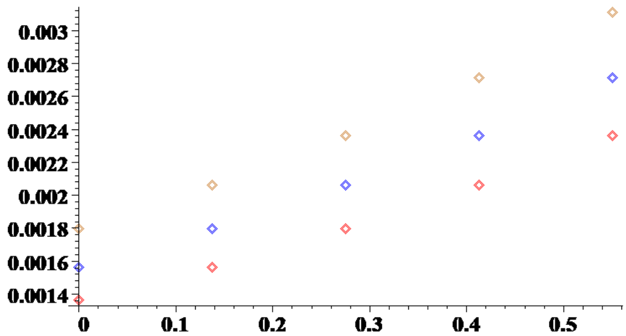

Fig. 6. The errors of the approximate solution at the nodes when we use polynomial splines, n=8, Digits=20, $\mathrm{cond}(A) = 1740$.
Source: created by the authors

Figure 7 shows the errors when $j = 1$ (red points), $j = 2$ (blue points), and $j = 3$ (gold points) when using basis exponential splines $\exp(x)$, $\exp(-y)$, when n =8, Digits=20. Figure 8 shows the errors when $j = 1$ (red points), $j = 2$ (blue points), and $j = 3$ (gold points) when using basis exponential splines $\exp(-x)$, $\exp(-y)$, when n =8, Digits=20. Figure 9 shows the errors when $j = 1$ (red points), $j = 2$ (blue points), and $j = 3$ (gold points) when using basis exponential splines $\exp(-x)$, $\exp(-y)$, when n =8, Digits=15.

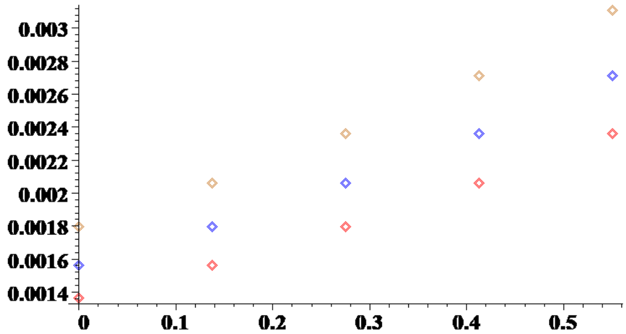

Fig. 7. The errors of the approximate solution at the nodes when we use exponential splines ($exp(x)$ and $exp(-y)$, n = 8, Digits=20, $cond(A) = 1699$.
Source: created by the authors

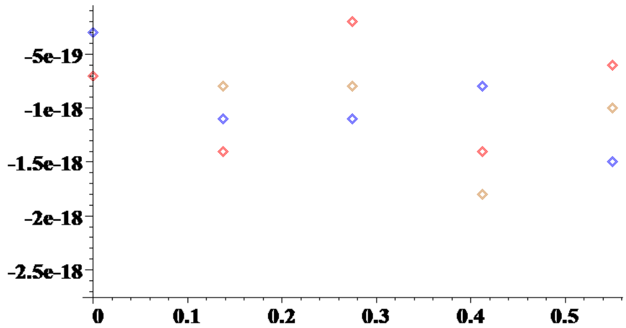

Fig. 8. The errors of the approximate solution at the nodes when we use exponential splines ($\exp(-x)$ and $\exp(-y)$, n = 8, Digits=20, $cond(A) = 1702$.
Source: created by the authors

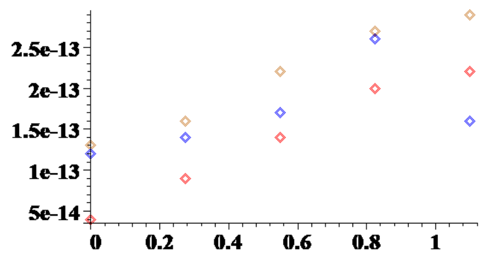

Fig. 9. The errors of the approximate solution at the nodes when we use exponential splines, n = 4, Digits=15.
Source: created by the authors

The maximum of the solution error is 0.18×10^{-2} in paper, [20], when 25 nodes were used. The maximum of the solution error is 0.81×10^{-5} in paper, [20], when 100 nodes were used.

Our method gives the error of the solution 0.32×10^{-1} when polynomial splines and 25 nodes were used. But when we use the exponential splines, the maximum error of the solution is 0.4×10^{-12} when 25 nodes were used and Digits=15 in Maple.
Using a two-dimensional spline approximation, we can quickly calculate the solution value at any point in the solution domain.
Example 2. Consider the equation from paper, [20]

$$2u(x,y) + \int_0^{1.1}\int_0^{1.1} \cos(x+y-s-t)u(s,t)dsdt = f(x,y),$$

where $u(x,y) = \sin(x+ y)$ is the exact solution and

$$f(x,y) = \frac{1}{2}\big(-0.125\sin(-x-y) + 0.25\sin(2.2-x-y) - 0.125\sin(4.4-x-y) + 2.605\sin(x+y)\big).$$

Figure 10 shows the errors when $j = 1$ (red), $j = 2$ (blue), and $j = 3$ (gold) points when using basis polynomial splines. Figure 11 shows the errors when $j = 1$ (red points), $j = 2$ (blue points), and $j = 3$ (gold points) when using basis polynomial splines.

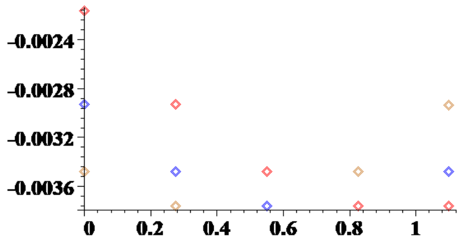

Fig. 10. The errors of the approximate solution at the nodes when we use polynomial splines, $n = 4$.
Source: created by the authors

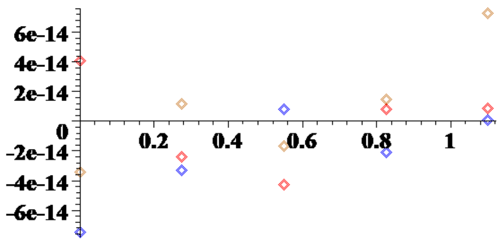

Fig. 11. The errors of the approximate solution at the nodes when we use trigonometrical splines, $n = 4$.
Source: created by the authors

The maximum of the solution error is 0.26×10^{-3} when 25 nodes were used in the paper, [20]. The maximum of the solution error is 0.45×10^{-3} when 100 nodes were used in the paper, [20].
Our method gives the error of the solution 0.37×10^{-2} when polynomial splines and 25 nodes were used. But when we use the trigonometrical splines, the error of the solution is 0.7×10^{-14} when 25 nodes and Digits=15 in Maple were used.

Example 3. Next, we solve an example from the paper, [21]. In the paper, [21], an expansion method, based on orthogonal polynomials, is developed to find numerical solutions of two-dimensional linear Fredholm integral equations.

$$u(x,y) - \int_{-1}^{1}\int_{-1}^{1} (x\sin(y) + s\exp(t))\,u(s,t)ds\,dt = x\exp(-y) + 4x\sin(y) - \frac{7}{3},$$

where the exact solution is the following: $u(x,y) = x\exp(-y) - 1$.
Table 3 and Table 4 show the results of numerical calculations in the MAPLE system. The columns show the maximum error of the approximate solution when using polynomial and non-polynomial splines, as well as the condition numbers of the system matrix.
The figures show the solution errors when using polynomial and non-polynomial splines.
Figure 12 shows the solution errors when using polynomial and exponential splines (with a negative parameter), $n = 4$.
Figure 13 shows the solution errors when using polynomial and exponential splines (with a positive parameter), $n = 4$.
Figure 14 shows the solution errors when using polynomial splines along both X and Y, $n = 4$.
Figure 15 shows the solution errors when using polynomial and exponential splines (with a positive parameter), $n = 4$, Digits=3.
Figure 16 shows the solution errors when using polynomial splines along both X and Y, $n = 4$, Digits=5.

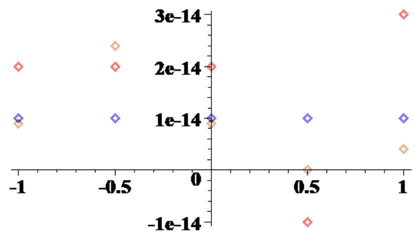

Fig. 12. The solution errors when using polynomial and exponential splines (with a negative parameter), $n = 4$, Digits=15.
Source: created by the authors

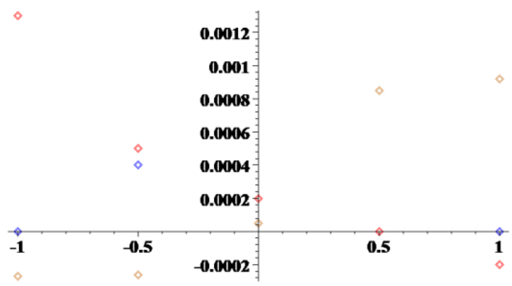

Fig. 13. The solution errors when using polynomial and exponential splines (with a negative parameter), $n = 4$, Digits=5.
Source: created by the authors

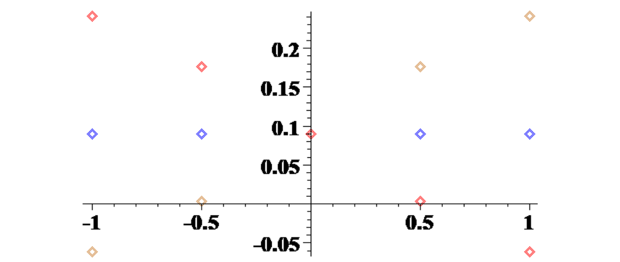

Fig. 14. The solution errors when using polynomial and exponential splines (with a positive parameter), $n = 4$, Digits=15.
Source: created by the authors

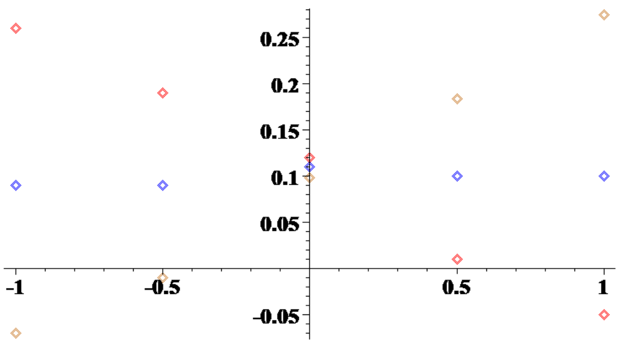

Fig. 15. The solution errors when using polynomial and exponential splines (with a positive parameter), $n = 4$, Digits=3.
Source: created by the authors

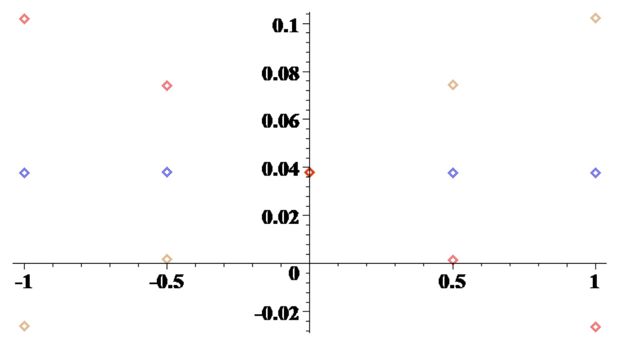

Fig. 16. The solution errors when using polynomial splines along both X and Y, $n = 4$, Digits=5.
Source: created by the authors

The values of the condition numbers of a matrix when applying polynomial splines in both directions ($\mathrm{pol}(x) \times \mathrm{pol}(y)$), polynomial splines along the X-axis and exponential splines ($\exp(y)$) along the Y-axis ($\mathrm{pol}(x) \times \exp(y)$), polynomial splines along the X-axis and exponential splines ($\exp(-y)$) along the Y-axis ($\mathrm{pol}(x) \times \exp(-y)$),

Table 3. Values of the condition numbers of the matrix A (*Examples 1,3*, $n = 4, 25$ equations)

	$\mathrm{pol}(x) \times \mathrm{pol}(y)$	$\mathrm{pol}(x) \times \exp(y)$	$\mathrm{pol}(x) \times \exp(-y)$
Example 3 Digits=*15*	74	86	65
Example 3 Digits=*5*	74	86	65
Example 1 Digits=*15*	4	4	4
Example 1 Digits=*5*	4	4	4

Source: created by the authors

Table 4. Values of the condition numbers of the matrix A (*Example 1*, $n = 8, 81$ equations)

	$\mathrm{pol}(x) \times \mathrm{pol}(y)$	$\mathrm{pol}(x) \times \exp(y)$	$\mathrm{pol}(x) \times \exp(-y)$
Example 1 Digits=*20*	1740	1702	1699

Source: created by the authors

Table 3 and Table 4 show that the condition number of the matrix grows with increasing number of grid nodes.

4 Conclusion

This paper discusses the construction of a numerical method for solving an integral equation from two variables using local splines. The advantages of solving integral equations using local polynomial and non-polynomial splines include the ease of using an adaptive non-uniform grid, as well as the ability to use different types of spline approximations, such as exponential or trigonometric, in each direction. Using appropriate non-polynomial splines can significantly reduce the solution error. Using a two-dimensional spline approximation, one can quickly calculate the solution values at any point in the solution domain.
In future papers, we will continue to explore the application areas of spline approximations for solving Fredholm integral equations. In the future, we plan to discuss in more detail the issues of stability and approximation for various non-polynomial spline options in a two-dimensional domain and in a three-dimensional domain.

Acknowledgement:
The authors are grateful to the St. Petersburg State University Resource Center for the opportunity to carry out calculations in MAPLE (project ID 135736503).

References:

[1] Sevastianov L. A., Lovetskiy K. P., Kulyabov D. S., Sergeev S. V, Numerical solution of first-order exact differential equations by the integrating factor method, Izvestiya of Saratov

University. *Mathematics. Mechanics. Informatics*, Vol. 24, No. 4, 2024, pp. 512–525. https://doi.org/10.18500/1816-9791-2024-24-4-512-525.

[2] Lovetskiy K. P., Kulyabov D. S., Hissein A.W., Multistage pseudo-spectral method (method of collocations) for the approximate solution of an ordinary differential equation of the first order, *Discrete and Continuous Models and Applied Computational Science*, Vol. 30, No. 2, 2022, pp. 127–138. https://doi.org/10.22363/2658-4670-2022-30-2-127-138

[3] Lovetskiy K. P., Sergeev S. V., Kulyabov D. S., Sevastianov L. A., Application of the Chebyshev collocation method to solve boundary value problems of heat conduction, *Discrete and Continuous Models and Applied Computational Science*, Vol. 32, No. 1, 2024, pp. 74–85. doi:10.22363/2658-4670- 2024-32-1-74-85. https://doi.org/10.22363/2658-4670-2024-32-1-74-85

[4] Khapaev M. M., Numerical Solution of an Integro-Differential Equation for a Sheet Current, *Differential Equations*, Vol. 41, 2005, pp. 1019–1024. doi:10.1007/s10625-005-0243-x. https://link.springer.com/article/10.1007/s10625-005-0243-x [Access Date: 01/01/2026]

[5] Mirzaee F., Samadyar N., Application of Bernoulli wavelet method for estimating a solution of linear stochastic Itˆo–Volterra integral equations, *Multidiscipline Modeling in Materials and Structures*, Vol. 15, No. 3, 2019, pp. 575–598. doi:10.1108/MMMS-04-2018-0075. https://www.emerald.com/mmms/article-abstract/15/3/575/294645/Application-of-Bernoulli-wavelet-method-for?redirectedFrom=PDF [Access Date: 01/01/2026]

[6] Cerna D., Finek V., Galerkin method with new quadratic spline wavelets for integral and integro-differential equations, *Journal of Computational and Applied Mathematics*, Vol. 363, 2020, pp. 426–443. doi:10.1016/j.cam.2019.06.033. https://dspace.tul.cz/items/34004b10-48f7-44fb-b5e5-d5a282dbca2c

[7] Mirzaee F., Alipour S., An efficient cubic B-spline and bicubic B-spline collocation method for numerical solutions of multidimensional nonlinear stochastic quadratic integral equations, *Mathematical Methods in the Applied Sciences*, Vol. 43, No. 1, 2019, pp. 384–397. doi:10.1002/mma.5890. https://onlinelibrary.wiley.com/doi/abs/10.1002/mma.5890 [Access Date: 01/01/2026]

[8] Assari P., Asadi-Mehregan F., Dehghan M. The implication of local thin plate splines for solving nonlinear mixed integro-differential equations based on the Galerkin scheme, *Numerical Mathematics: Theory, Methods and Applications*, Vol. 12, No. 4, 2019, pp. 1066–1092. doi:10.4208/nmtma.OA2018-0077. https://www.researchgate.net/publication/334635582_The_Implication_of_Local_Thin_Plate_Splines_for_Solving_Nonlinear_Mixed_Integro-Differential_Equations_Based_on_the_Galerkin_Scheme [Access Date: 01/01/2026]

[9] Graham I. G., Collocation methods for two dimensional weakly singular integral equations, *Journal of the Australian Mathematical Society: Series B, Applied Mathematics*, Vol. 22, No. 4, 1981, pp. 456–473. https://pascal-francis.inist.fr/vibad/index.php?action=getRecordDetail&idt=PASCAL8130482706 [Access Date: 01/01/2026]

[10] McKee S., Tang T., Diogo T., An Euler-type method for two-dimensional Volterra integral equations of the first kind, *IMA Journal of Numerical Analysis*, Vol. 20, No. 3, 2000, pp. 423–440. DOI:10.1093/imanum/20.3.423 https://www.researchgate.net/publication/265367866_An_Euler-type_method_for_two-dimensional_Volterra_integral_equations_of_the_first_kind [Access Date: 01/01/2026]

[11] Engeln–M¨ullges G., Uhlig F., *Numerical Algorithms with C.*, Berlin, Heidelberg: Springer, 1996. 610 p. ISBN 3642646824, 9783642646829 https://books.google.ru/books/about/Numerical_Algorithms_with_C.html?id=KGfvCAAAQBAJ&redir_esc=y [Access Date: 01/01/2026]

[12] Farengo R., Lee Y. C., Guzdar P. N., An electromagnetic integral equation: application to microtearing modes, *Physics of Fluids*, Vol. 26, No. 12, 1983, pp. 3515–3523. doi:10.1063/1.864112. https://pubs.aip.org/aip/pfl/article-abstract/26/12/3515/809067/An-electromagnetic-integral-equation-Application?redirectedFrom=fulltext [Access Date: 01/01/2026]

[13] Atkinson K. E., Chien D. D., Seol J., Numerical analysis of the radiosity equation using the collocation method, *Electronic Transactions on Numerical Analysis*, Vol. 11, 2000, pp. 94–120. https://www.researchgate.net/publication/2856

85150_Numerical_analysis_of_the_radiosity_equation_using_the_collocation_method [Access Date: 01/01/2026]

[14] Atkinson K. E., *The Numerical Solution of Integral Equations of the Second Kind*. Cambridge: Cambridge University Press, 1997. 571 p. ISBN: 9780511626340 https://doi.org/10.1017/CBO9780511626340 https://www.cambridge.org/core/books/numerical-solution-of-integral-equations-of-the-second-kind/91E77DDA93701D3B024830429043A037 [Access Date: 01/01/2026]

[15] Atkinson K. E., Numerical solution of Laplace's equation in three dimensions. SIAM *Journal on Numerical Analysis*, Vol. 19, No. 2, 1982, pp. 263–274. doi:10.1137/0719017. https://www.researchgate.net/publication/258915802_The_Numerical_Solution_of_Laplace's_Equation_in_Three_Dimensions [Access Date: 01/01/2026]

[16] Liu H., Huang J., Pan Y., Numerical Solution of Two Dimensional Fredholm Integral Equations of the Second Kind by the Barycentric Lagrange Function, *Journal of Applied Mathematics and Physics*, Vol. 5, 2017, pp. 259–266. doi:10.4236/jamp.2017.52023. https://www.scirp.org/journal/paperinformation?paperid=74145 [Access Date: 01/01/2026]

[17] Ma Y., Huang J., Li H., A Novel Numerical Method of Two-Dimensional Fredholm Integral Equations of the Second Kind, *Mathematical Problems in Engineering*, 2015, Vol. 2025, No. 1, Article ID 625013. doi:10.1155/2015/625013. https://onlinelibrary.wiley.com/doi/10.1155/2015/625013 [Access Date: 01/01/2026]

[18] Wen-Jing X., Fu-Rong L. A fast numerical solution method for two dimensional Fredholm integral equations of the second kind. Applied Numerical Mathematics, Vol. 59, No. 7, 2009, pp. 1709–1719. doi:10.1016/j.apnum.2009.01.009. https://www.sciencedirect.com/science/article/abs/pii/S0168927409000117 [Access Date: 01/01/2026]

[19] Burova I. G., On left integro-differential splines and Cauchy problem, *International Journal of Mathematical Models and Methods in Applied Sciences*, Vol. 9, 2015, pp. 683–690. ISSN: 1998-0140 https://www.naun.org/main/NAUN/ijmmas/2015/b582001-015.pdf [Access Date: 01/01/2026]

[20] Khaksari N., Paripour M., Karamikabir N., Numerical Solution for the 2D Linear Fredholm Functional Integral Equations, *Journal of Mathematics*, 2021, Vol. 12, Article ID 9560595. doi:10.1155/2021/9560595 https://www.researchgate.net/publication/356117275_Numerical_Solution_for_the_2D_Linear_Fredholm_Functional_Integral_Equations [Access Date: 01/01/2026]

[21] A. Tari, S. Shahmorad, A Computational Method for Solving Two-Dimensional Linear Fredholm Integral Equations of the Second Kind, *ANZIAM J.*, 49, 2008, 543–549, doi:10.1017/S1446181108000126 https://www.cambridge.org/core/journals/anziam-journal/article/computational-method-for-solving-twodimensional-linear-fredholm-integral-equations-of-the-second-kind/DE36FF437743C20BDA74E80FA86F4447 [Access Date: 01/01/2026]

Contribution of Individual Authors to the Creation of a Scientific Article (Ghostwriting Policy)

I. G. Burova was responsible for the theoretical results and carried out the simulation, organized the experiments, and optimized the results.
G. O. Alcybeev has organized and executed the experiments.
S. A. Shipcova has organized and executed some experiments.

Sources of Funding for Research Presented in a Scientific Article or Scientific Article Itself

No funding was received for conducting this study.

Conflict of Interest

The authors have no conflicts of interest to declare that are relevant to the content of this article.